Electronic and magnetic structure of the Cr(001) surface.

Cyrille Barreteau, Parwana Habibi, Alexander Smogunov

Electronic and magnetic structure of the Cr(001) surface.

P. Habibi

CEA, IRAMIS, SPCSI, 91191 Gif-sur-Yvette Cedex, France

C. Barreteau

CEA, IRAMIS, SPCSI, 91191 Gif-sur-Yvette Cedex, France

A. Smogunov

CEA, IRAMIS, SPCSI, 91191 Gif-sur-Yvette Cedex, France

E-mail: cyrille.barreteau@cea.fr

Abstract. Density Functional Theory (DFT) calculations are carried out to study the electronic and magnetic structure of the (001) surface of Chromium. Our aim is to identify and characterize the most prominent electronic surface states and make the connection with the main experimental results. We show that a low dispersive minority spin surface state at the center of the Surface Brillouin zone plays a crucial role. This surface state of Δ_1 symmetry at 0.58eV above the Fermi level exhibits predominantly a d_{z^2} as well as p_z orbital character. Local density of states (LDOS) analysis in the vacuum above the surface shows that the sharp feature originating from this surface state persists far away above the surface because of the slow decay rate of p_z wave function. Finally by artificially lowering the surface magnetic moment $\overline{m}_S$ on the outermost surface layer we find an excellent agreement with experiments for $\overline{m}_S = 1.75\mu_B$. In addition we propose that some extra Spin Polarized Scanning Tunneling Spectroscopy (SP-STS) experiments should be made at smaller tip-surface distances to reveal additional features originating from the majority spin d_{z^2} surface state.

PACS numbers: 73.20.At, 71.15.Mb, 75.10.Lp, 75.50.Ee, 75.70.Ak

1. Introduction

Chromium is a rather fascinating element with unusual magnetic properties and used in many technological applications in domains as different as metallurgy or spintronic devices based on magnetic multi-layers. Its simple crystallographic body centered cubic (bcc) structure contrasts with the complexity of its magnetic ordering. Indeed the magnetic ground state of Cr is the so-called spin-density wave[1] (SDW) which can be described as a long (incommensurate) period modulating the amplitude of the magnetic moment along the $\langle 001 \rangle$ direction. Although very well established experimentally the theoretical description of the SDW is still unsatisfactory[2, 3]: this magnetic arrangement is usually attributed to nesting properties of the Fermi surface but calculations based on Density Functional Theory (DFT) formalism or Tight-Binding (TB) model never predict the SDW as the ground state. It is found either non magnetic or anti-ferromagnetic depending on the exchange correlation functional[3], the commensurate SDW approximating the real magnetic order being always slightly higher in energy. In addition the magnetic moment found when using the Generalized Gradient Approximation (GGA) exchange-correlation functional is largely overestimated compared to experiment ($1.2\mu_B$ instead of $0.59\mu_B$)

The symmetry breaking induced by the presence of a surface authorizes, for certain orientations, the creation of a net magnetic moment at the surface of Chromium since the magnetic moments of adjacent atomic planes parallel to the surface do not need to cancel each other. It was recognized theoretically already in the 1970's that the Cr(001) surface is ferromagnetic with a huge surface magnetic moment as large as $3\mu_B$[4]. From an experimental point of view the situation is a bit confusing since some discrepancies between band structure calculations and angle resolved photoelectron spectroscopy[5] experiments were pointed that were partly attributed to an overestimation of the surface magnetization in DFT. Later on tunneling spectroscopy experiments[6] showed again that an agreement between experiment and theory cannot be obtained without a reduction of surface magnetization.

The surface of Chromium has also been one of the favorite system for the development of spin-polarized scanning tunneling microscopy (SP-STM)[7]. In particular the (001) surface is an ideal template to visualize magnetic order at the atomic scale since, due to the local anti-ferromagnetic coupling between neighboring atoms, adjacent terraces show opposite magnetic orientation which contrast appears clearly in SP-STM. The improvement in SP-STM technology (as well as surface preparation) and in particular the use of real space spectroscopy imaging at low temperature has allowed to provide a detailed characterization of the spin polarized electronic structure of chromium surface. In 2002 Kolesnychenko *et al*[8] observed sharp features in the tunneling spectroscopy (STS) at the Fermi level which they attributed to an orbital Kondo resonance[8, 9] formed by two degenerate d_{xz} d_{yz} surfaces states located, according to their electronic structure calculations, around -1eV ($+1$ eV) below (above) the Fermi level for up (down) spins. Later on Budke *et al* performing combined STS,

photo-emission and inverse photo-emission experiments[10] put forward some strong arguments in favor of d_{z^2}-like (Δ_1 symmetry) surface state interpretation for the peak at the Fermi level. Nowadays the physical origin of this state is still contoversial[11].

In this paper we present results of DFT electronic structure calculations to analyze in detail the spin dependent band structure of the (001) surface of Chromium. We have found in agreement with previous calculations that the magnetic moment of the outermost layer is strongly amplified. We have also identified and characterized the most important surface states in particular the ones in the vicinity of the Fermi level. The principal features of the surface projected density of states already described in the literature are recovered but we go a step further by providing the full $\boldsymbol{k}$ resolved surface band structure and the orbital character of all the surface states. In addition the investigation of the surface projected density of states (PDOS) in combination with local density of states in the vacuum allow us to highlight the important role of a minority spin surface state of p_z d_{z^2} orbital character persisting far away above the surface which we believe is at the origin of the sharp feature observed experimentally.

2. Methodology

2.1. Density Functional Therory (DFT) calculations

The present DFT calculations have been performed within density functional theory as implemented in the Quantum Espresso package[12]. This code is based on a plane wave expansion of the wave functions and the effect of the core electrons on the valence electrons is taken into account by the use of ultrasoft pseudo-potentials. All our results were obtained within the generalized gradient approximation (GGA) and the Perdew-Burke-Ernzehof (PBE) form of the exchange correlation functional.

The calculation are spin polarized in a collinear formalism and spin-orbit coupling is neglected. The plane wave expansion implies a three-dimensional periodicity that can produce spurious interaction between elementary unit cells and one has to use the super-cell technique by introducing a sufficient "empty space" to avoid unphysical interactions between periodic images. In this work we have essentially studied the (001) surface of bcc Chromium which is described in a slab geometry with an empty space between two adjacent slabs of 12Å. The $\boldsymbol{k}$ points grid was $20 \times 20 \times 20$ for bulk bcc and $20 \times 20 \times 1$ for slabs of 19 atomic layers. A Methfessel Paxton broadening scheme with 0.15eV broadening width was used.

2.2. Projected and Local Density of states

In this study we have used two types of local analysis of the electronic density of states. A first one called Projected Density States (PDOS) is based on a Löwdin projection of the density of states onto pseudo-atomic wave functions. The second one called Local Density of States (LDOS) is a spatial representation of the density of states in a given region of space.

Let us call $\hat{D}(E) = \delta(E - \hat{H})$ the density operator of Hamiltonian $\hat{H}$ which takes the simple diagonal form in its eigen-basis $\sum_\alpha |\Psi_\alpha\rangle\delta(E-\varepsilon_\alpha)\langle\Psi_\alpha|$. The PDOS on the atomic orbitals $|\phi_{i,\lambda}\rangle$ ($\lambda = s, p_x, p_y, p_z, d_{xy}, d_{yz}, d_{xz}, d_{x^2-y^2}, d_{3z^2-r^2}$) centered on atom i is given by:

$$D_{i,\lambda}(E) = \sum_\alpha |\langle\phi_{i\lambda}|\Psi_\alpha\rangle|^2\delta(E-\varepsilon_\alpha) \tag{1}$$

Integrating this equation over the energy up to the Fermi level and summing over the atomic orbitals permit to define local charges n_i and magnetic moments m_i. In fact the derived expressions must be slightly modified to account for the overlap between the atomic orbital. The partition of "electrons" between neighboring atoms depends on an arbitrary choice (Mulliken or Löwdin). Note also that the summation over $\alpha = (\boldsymbol{k}, n)$ index includes the $\boldsymbol{k}$ space sampling of the Brillouin zone as well as the discrete summation over the energy bands. It can also be of interest to define a $\boldsymbol{k}$ resolved density of states for specific vectors in the Brillouin zone.

The LDOS is equivalently written in the eigen-basis:

$$D(E,\boldsymbol{r}) = \langle r|\hat{D}(E)|\boldsymbol{r}\rangle = \sum_\alpha |\Psi_\alpha(\boldsymbol{r})|^2\delta(E-\varepsilon_\alpha) \tag{2}$$

$D(E,\boldsymbol{r})$ can also be integrated over a given region of space such as a sphere S_i centered on a given atom i. If the sphere is sufficiently large (but non-overlapping with the neighbouring ones) the integrated LDOS should be very close to the PDOS summed up over the relevant atomic orbitals of the corresponding atom. An additionnal integration over the energy range up to the Fermi level gives an alternative definition of local charges and magnetic moments which will be noted $\overline{m}_i$. More sophisticated partitions based on Bader analysis[13] are also sometimes found in the literature.

LDOS will be used in this paper to analyze the density of states at various distances above the surface. In that context it is interesting to rewrite $D(E,\boldsymbol{r})$ introducing the pseudo-atomic basis set:

$$D(E,\boldsymbol{r}) = \sum_{\substack{i,\lambda\\ j,\mu}} \phi_{i\lambda}(\boldsymbol{r})\phi^*_{j\mu}(\boldsymbol{r}) \sum_\alpha \langle\phi_{i\lambda}|\Psi_\alpha\rangle\langle\Psi_\alpha|\phi_{j\mu}\rangle\delta(E-\varepsilon_\alpha) \tag{3}$$

Due to the localized character of the atomic wave functions and their different decay rates it can happen that a given atom i_0 and orbital λ_0 is dominating this sum and $D(E,\boldsymbol{r})$ then takes a simpler form:

$$D(E,\boldsymbol{r}) \approx \sum_\alpha |\phi_{i_0\lambda_0}(\boldsymbol{r})|^2|\langle\phi_{i_0\lambda_0}|\Psi_\alpha\rangle|^2\delta(E-\varepsilon_\alpha) = |\phi_{i_0\lambda_0}(\boldsymbol{r})|^2 D_{i_0,\lambda_0}(E) \tag{4}$$

In that limit the LDOS can be simply related to the PDOS. This kind of situation typically occurs for large distances away from the surface relevant in STM experiments.

3. Results and discussion

3.1. Band structure of bulk Chromium

The bulk density of states (DOS) of AF Chromium is characteristic of the DOS of bcc materials with its well known pseudo gap around the Fermi level. In fact the effect of magnetism is rather small on the overall shape of the DOS[14, 3]. The main difference is the presence of a small peak 0.2eV below the Fermi level due to the mechanism of gap opening which participates to the stabilization of the AF solution (see discussion below).

The band-structure of Chromium can be understood from the non magnetic state (see top panel of Fig. 1). As explained by Kübler[15] one should start by folding the nonmagnetic (NM) band-structure of the bcc Brillouin zone into the simple cubic (sc) Brillouin zone appropriate for the CsCl structure needed in the case of AF Chromium. The effect of the AF arrangement (with alternating "up" and "down" atomic sites) leads to the well known gap opening and degeneracy lifting along high symmetry direction or at zone boundaries. Along ΓM and ΓR there is a clear avoided-crossing which produces two inverted parabolas 0.2eV below the Fermi level (see bottom panel of Fig. 1). Along the ΓX direction (see Fig. 2) there are three important gap opening at the X point for the bands of Δ_2, Δ_2' and Δ_5 symmetry. The one of Δ_5 symmetry is particularly noticeable since the upper branch is pushed above the Fermi level while the lower one becomes almost non-dispersive. The symmetry of the bands (see Table 1) will also be useful in the discussion concerning surface states. As already pointed out by by Enkovaara *et* al.[16] there are no bands of Δ_1 symmetry in the vicinity of Fermi level (note however that in Figure 1 of their paper the two lowest lying bands Δ_1 and Δ_5 should be inverted).

representation	basis function	E	C_2	$2C_4$	$2\sigma_v$	$2\sigma_d$
Δ_1	$1, z, z^2$	1	1	1	1	1
Δ_2	$x^2 - y^2$	1	1	-1	1	-1
Δ_2'	xy	1	1	-1	-1	1
Δ_1'	$xy(x^2 - y^2)$	1	1	1	-1	-1
Δ_5	$x, y; zx, zy$	2	-2	0	0	0

Table 1. Character table of the C_{4v} group for a wave vector $\mathbf{k}$ along the $\Delta = \frac{2\pi}{a}(00x)$ axis.

3.2. (001) surface of Chromium

In the following we will present results of our DFT calculations on the (001) surface of Chromium in its anti-ferromagnetic phase. By convention the magnetization of the outermost surface layer will be taken as the "up" spin direction which corresponds to the so-called majority spin. We are aware that AF is not the ground state of Chromium,

however it was shown that the electronic PDOS and magnetization in the vicinity of the (001) surface are almost identical between AF order or an out-of-plane SDW[17]. In addition we have also verified, by carrying out additional calculations within the tight-binding scheme presented in Ref.[3] for a slab containing up to 41 atomic layers in presence of an out-of-plane SDW, that the position and dispersion of the surface states are almost unchanged with respect to the antiferromagnetically ordered slab. Therefore we are confident that all the conclusions derived below are perfectly transferable to the case of a SDW order.

Let us also mention that we have optimized all the atomic positions and found rather modest surface relaxations (interlayer contraction between the two topmost atomic planes is below 5%) as already stated in one of our previous publications[17]. In consequence the surface electronic and magnetic structure is almost unaffected by the relaxation. Our findings are very similar to results obtained with the full-potential linearized augmented plane-wave (FLAPW) method[2]. Note however that two other publications[18, 19] relate strong surface relaxations. The discrepancy between their results (obtained with the same DFT code in a projected augmented wave formalism) and most other works may be attributed to the fact that their bulk magnetic moment is rather small ($\pm 0.59\mu_B$) compared to other GGA calculations. In contrast, another publication[20] by the same group as Ref.[18] finds magnetic moments in very good agreement with us (around $\pm 1\mu_B$ depending on the lattice parameter). This proves that magnetism of Chromium is indeed a delicate subject.

3.2.1. Surface magnetic moment. Magnetism is usually reinforced at surface sites due to a narrowing of the density of states for atoms with lower coordination. Cr is rather interesting due to its AF order which is locally broken at the (001) surface. Indeed the spin moment at the surface site does not need to be compensated by the one of the sub-surface and a net magnetization is allowed. In the case of Cr(001) this effect is particularly drastic (see Fig. 3) since at the surface the Löwdin spin moment reaches $m_S = 3\mu_B$ almost two and a half times the bulk value $m_{\text{bulk}} = \pm 1.27\mu_B$. The sub-surface atom bears an opposite magnetic moment of -1.80μ_B. The sum over the 4 first surface layers gives a net magnetic moment of $1.32\mu_B$. It is worth mentionning that when using a different definition of the atomic moment by integrating the spin density over an atomic sphere, the local moments found differ significantly from the Löwdin definition. This is particularly pronounced at the surface since $\overline{m}_S = 2.49\mu_B$ while in the bulk the difference is much smaller $\overline{m}_{\text{bulk}} = \pm 1.11\mu_B$.

As pointed out by Soulairol *et al* [17] this large enhancement of the surface spin moment contributes to a stabilization of the (001) surface which is lower in energy than the (110) in contradiction with the usual argument which states that the densest surface has the lowest surface energy. One can also note that the chemical elements Mo and W which are in the same column of the periodic table as Cr both present a reconstruction of the (001) surface attributed to the presence of a large peak at the Fermi level of the surface PDOS. In the case of Chromium the surface instability seems to be lifted by

magnetism.

3.2.2. Band structure. The surface band structure provides a detailed picture of the quantum states since it reflects not only the bulk dispersion (projected bulk band structure) with eventual presence of "pseudo"-gaps but can also reveal the existence of surface states which $\boldsymbol{k}$ space extension is usually limited to these gaps, transforming into surface resonances when entering into the bulk continuum. Fig. 4 is showing the band-structure of a 19 layers slabs. For the sake of clarity and to facilitate the discussion hereafter we have labeled the most important surface states.

From Figs 4 it is clear that most states are essentially of spin up character (S_1, $\cdots$,S_4, S_Γ). Only states S_5, S_6 and S'_Γ (around the $\overline{\Gamma}$ point) have a spin down character. The prominent low dispersive surface states and therefore contributing the most significantly to the surface LDOS are S_1, S'_1, S'_2, and S'_Γ . The orbital character of surface states greatly influences their physical behavior: For example surface states with a strong d character will respond more significantly to surface magnetism than those of s or p character. This is the case of S_1 which is almost purely d and therefore much more sensitive to the surface magnetization than S_2, S'_2 or S_3 states having a certain weight on p orbitals. In addition the extension of surface states into vacuum depends on their orbital character which impacts on the ability of being detected via STM experiment. To illustrate this phenomenon we have represented on Fig. 5 the square of the Bloch function corresponding to states S_1 and S'_Γ along a line going away from the surface and originating from a surface atom. It is clear that the surface state S'_Γ leaks much further away from the surface than state S_1. This is due to the strong p_z character of S'_Γ while S_1 is dominantely of d_{z^2} character.

By calculating the weight of the eigenfunctions on atomic orbitals of surface sites (*i.e.* $|\langle\phi_{i\lambda}|\Psi_\alpha\rangle|^2$) we have been able to obtain a detailed picture of the dominant character of each surface state. A handy representation consists in plotting the surface band-structure where the size of the spots is proportional to the surface weight on a given orbital. Figs. 6 show an example of such orbital projected band-structure on d_{z^2} and p_z orbitals. The four low dispersive states S_1, S'_1, S'_2, and S'_Γ have a dominant d_{z^2} character and will contribute to the PDOS around the Fermi level as discussed in next section. S'_2 and S'_Γ have also an important p_z component. S_3 have a common p_z-d_{z^2} character as well but is much more dispersive and will contribute modestly to the surface density of states. It is also worth mentionning that there are few true d_{xz} and d_{yz} surface states. In addition most of them are either stongly dispersive (S_2) or have a non neglible weight on bulk sites (and therefore are resonant states).

Let us now discuss more specifically the case of surface states at $\overline{\Gamma}$ point: S_Γ and S'_Γ. A detailed analysis using a $\boldsymbol{k} = \overline{\Gamma}$-resolved projected density of states reveals that S_Γ is in fact made of two majority spin surface states: one of Δ_1 symmetry at -1.05 eV with equivalent p_z and d_{z^2} weight and another one of Δ_5 symmetry at -0.97eV essentially of d_{xz}, d_{yz} character. S'_Γ is a minority spin surface state of Δ_1 symmetry at $0.58eV$ above E_F also with an equivalent p_z and d_{z^2} weight. The two Δ_1 surface states clearly appear

S_1	S_1'	S_2	S_2'	S_3	S_4	S_5	S_6	$S_\Gamma(\times 2)$	S_Γ'
d_{z^2}	d_{z^2}	$d_{xz}\ d_{yz}\ p_x$	$p_z\ d_{z^2}$	$d_{xz}\ p_z\ s$	$d_{x^2-y^2}\ s$	d_{xy}	$d_{x^2-y^2}\ s$	$p_z\ d_{z^2}$ / $d_{xz}\ d_{yz}$ Δ_1 / Δ_5	$d_{z^2}\ p_z\ s$ Δ_1

Table 2. Dominant orbital character of the various Cr(001) surface states.

in a symmetry gap since no bulk states of same symmetry are present in this energy range (see Fig. 2). The Δ_5 state is situated just below the bottom of the flat band of same symmetry in the bulk. In Table 2) we have summarized the main contributions of the various orbitals to the surface states.

3.2.3. Projected Density of States. In this section we will examine the projected density of states on the (001) surface atom of Chromium. In Fig. 7 we have presented the PDOS of the Cr(001) surface decomposed into orbitals of d and p_z character (s, p_x and p_y are ignored since they do not show any noticeable features). Several prominent peaks are present in the density of states (especially for the d orbitals) which most often can be attributed to specific surface states. It is quite striking to notice that none of these peaks is present at the Fermi level. However there are two sharp peaks of d_{z^2} character in the vicinity of E_F denoted $S_1 + S_1' + S_2'$ and S_Γ'. The first one situated 0.2eV above E_F originates essentially from the "up" spin surfaces states S_1, S_1' and S_2' clearly visible in the pseudo-gap of the surface band structure of Figs. 6, while the second one $0.58eV$ above E_F arises almost only from the down spin S_Γ' surface state. A rather peculiar feature of this latter state is that it couples strongly with p_z orbitals contributing to the formation of a peak in the surface p_z DOS as well. To compare more finely the PDOS of d_{z^2} and p_z character we have presented them on the same graph in panel a) of Fig. 7. It is indeed quite unusual to observe such a sharp feature in the PDOS of p_z orbital. In the next section we will see that it has some important consequences on the electronic density in the vacuum above the surface. On the contrary the contribution of the p_z orbital to the majority spin PDOS is much lower and spread over a large energy range in accord with the dispersion observed on the projected band structure (See Bottom panel of Fig. 6). Finally as already mentionned in previous publications [8, 9] the two degenerate $d_{xz}\ d_{yz}$ states show a peak at -1eV ($+1$ eV) below (above) the Fermi level for up (down) spins. However the detailed band structure analysis in the previous section tells us that the origin of these peaks is not due to localized surface states but rather by an assembly of resonance states.

3.2.4. Vacuum Density of States above the (001) *surface of Chromium* PDOS is a handy tool for the analysis of surface electronic structure however no experiment can provide a direct information on this quantity. In particular Scanning Tunneling Microscope is only probing the evanescent electronic density in the vacuum above the surface. Indeed in Tersoff-Hamman approach the tunneling differential conductance [21]

can be written:

$$G = \frac{\mathrm{dI}}{\mathrm{dU}} \propto \sum_{\sigma} D_T^{\sigma} D_S^{\sigma}(R, E_F + eU) \tag{5}$$

where D_T^{σ} is the spin-dependent tip PDOS (assumed to be constant in energy), and $D_S^{\sigma}(R, E)$ the spin-dependent vacuum LDOS of the surface at the tip position R. We have therefore investigated the vacuum LDOS of the Cr(001) surface at various positions R (ranging from $1\mathring{A}$ to $6.3\mathring{A}$) above the surface atom (position "on top"). This allowed us to study the decay of this quantity while moving away from the surface. Interestingly we noticed that for distances close to the surface the LDOS roughly resembles a combination of d_{z^2} and p_z PDOS whereas for larger distances only the p_z component remains (which is consistent with equation 4) as seen from the left panels of Fig. 8 where the LDOS at $z = 2.4\mathring{A}$ and $z = 5.1\mathring{A}$ are presented. This means that in the tunneling regime STM will preferentially probe these p_z-like states and we believe that the sharp feature observed experimentally by STS in the vicinity of the Fermi level is related to the S'_{Γ} surface state. It would however be useful to perform SP-STM (and STS) experiments at shorter tip-surface distances to probe d_{z^2}-like states that would reveal additional structures.

3.2.5. Sensibility to surface magnetization. To explain the discrepancies between experiment and theory and especially the existence of a sharp feature at E_F in the tunneling spectroscopy but not present in the calculation, people have mainly invoked two arguments: i) complex many-body electronic effects such as orbital-Kondo resonance or ii) overestimation of the calculated surface magnetization. This overestimation could have various origins: a mehodological problem related to the limitations of DFT or a more physical problem due to the presence of defects or impurities in experiment neglected in our calculation. For example it was shown by us in a recent publication[22] that the magnetization of surface atoms of chromium in contact with a C60 is drastically reduced and reach values below the bulk ones. There are now also some strong indications[10] essentially based on symmetry arguments in favor of a standard surface state of predominantly d_{z^2}-like character.

We have therefore performed a series of DFT calculations on the Cr(001) surface trying to impose a given surface magnetization. The method used is the so-called penalization technique[23] that consists in adding to the density functional a term $\lambda(\overline{m}_S - \overline{m}_S^0)^2$ proportional to the means square deviation of the surface magnetization $\overline{m}_S$ from its target value $\overline{m}_S^0$ (where λ is a large positive parameter). By trial and error we have come to the conclusion that a surface spin moment of $\overline{m}_S = 1.75\mu_B$ is a good estimate, the magnetic moment of the two sub-surface layers being $\overline{m}_{S-1} = -1.11$ and $\overline{m}_{S-2} = 1.17$ respectively. Note that the corresponding Löwdin surface moments are larger since $m_S = 2.15\mu_B$, $m_{S-1} = -1.29\mu_B$ and $m_{S-2} = 1.33\mu_B$.

On the right panels of Fig. 8 we show the LDOS in vacuum 2.4 and $5.1\mathring{A}$ above the (001) surface obtained from a DFT calculation where the magnetic moment $\overline{m}_S$ of the topmost layer has been constrained to $1.75\mu_B$. The position of the minority spin peak

has now been pushed down in energy from 0.58eV to 0.14eV. From the LDOS at 2.4$\mathring{A}$ it also appears that the majority bands (of dominant d character) are pushed up in energy of approximately the same amount. This is not so clearly visible at 5.1 $\mathring{A}$ since at this distance from the surface the LDOS mainly reflects the p orbitals which, for the majority spins, are weakly coupled to d orbitals. These results are in good agreement with recent SP-STS experiments[24] exhibiting the largest magnetic contrast at a bias voltage of 0.1eV corresponding to the position of the peak in the dI/dU spectra measured on the so-called "left terrace" (which we would attribute to a terrace of magnetization opposite to the STM tip). It is also found that the magnetic contrast is strongly bias-dependent in agreement with our findings since, away from its sharp feature, the LDOS of down spins is decreasing rapidly and becomes smaller than the one of up spins.

4. Conclusions

The aim of this study is to investigate by means of electronic structure calculations the energy band and magnetic structure of the Cr(001) surface. We have provided a very detailed description of the surface band structure and in particular we identified and characterized the most important surface states. It appears that the two degenerate d_{xz}, d_{yz} states invoked to explain the orbital Kondo mechanism[8, 9], even-though contributing to the surface density of states, are not strongly localized at the surface. On the contrary several low dispersive d_{z^2}-like surface states of majority spin character localized in large pseudo-gaps around the $\overline{M}$ point contribute to the formation of a sharp peak in the surface density of states 0.2eV above the Fermi level. In addition an almost flat minority spin d_{z^2}-like surface state around the $\overline{\Gamma}$ is also present 0.58eV above E_F. This state strongly coupled to p_z-like orbitals produces an unusually sharp feature in the p_z surface density of states. We show that this has important consequences on its ability to be detected by electron tunneling techniques. Indeed this peak (contrary to the one of d_{z^2} majority spin character) is persistent far away from the surface because of the slow decay rate of the p_z orbital. We suggest this is at the origin of the signal observed in STS spectra. In addition its position being 0.58eV higher in energy this is a strong indication of an overestimation of the surface magnetic moment from DFT calculations. Finally, performing constrained DFT calculations we could obtain an excellent agreement with recent SP-STS experiments for a surface magnetization of approximately $1.7\mu_B$.

Acknowledgments

We thank Alexandre Bataille, Marie-Alix Leroy, Vincent Repain and Jérôme Lagoute for helpful discussions and their expertise on the experimental aspects of ARPES and SP-STS measurements.

[1] E.. Fawcett. *Rev. Mod. Phy.*, 60:209, 1988.
[2] G. Bihlmayer, T. Asada, and S.. Blügel. *Phys. Rev. B*, 662:R11 937, 2000.
[3] R. Soulairol, Chu-Chun Fu, and C. Barreteau. *J. Phys. Condens. Matter*, 22(29):295502, 2010.
[4] G.. Allan. *Surf. Sci.*, 74:79, 1978.

[5] L.E. Klebanoff, R.H. Victoria, L.M. Falicov, and D.A. Shirley. *Phys. Rev. B*, 32:1997, 1985.
[6] A. Joseph Strocio, D.T. Pierce, A. Davies, R.J. Celotta, and M.. Weinert. *Phys. Rev. Lett.*, 75:2960, 1995.
[7] R. Wiesendanger, H.-J. Güntherodt, G. Güntherodt, R.J. Cambino, and R. Rut. *Phys. Rev. Lett.*, 65:247, 1990.
[8] O. Yu. Kolesnychenko, R. de Kort, M.I. Katselson, A.I Lichtenstein, and H. van Kempen. *Nature*, 415:507, 2002.
[9] O. Yu. Kolesnychenko, G.M. Heijnen, A.K. Zhuravlev, R. de Kort, M.I. Katselson, A.I Lichtenstein, and H. van Kempen. *Phys. Rev. B*, 72:085456, 2005.
[10] M. Budke, T. Allmers, M. Donath, and M.. Bode. *Phys. Rev. B*, 77:233409, 2008.
[11] T. Hänke, M. Bode, S. Krause, L. Berbil-Bautista, and R.. Wiesendanger. *Phys. Rev. B*, 72:085453, 2005.
[12] Paolo Giannozzi, Stefano Baroni, Nicola Bonini, Matteo Calandra, Roberto Car, Carlo Cavazzoni, Davide Ceresoli, Guido L Chiarotti, Matteo Cococcioni, Ismaila Dabo, Andrea Dal Corso, Stefano de Gironcoli, Stefano Fabris, Guido Fratesi, Ralph Gebauer, Uwe Gerstmann, Christos Gougoussis, Anton Kokalj, Michele Lazzeri, Layla Martin-Samos, Nicola Marzari, Francesco Mauri, Riccardo Mazzarello, Stefano Paolini, Alfredo Pasquarello, Lorenzo Paulatto, Carlo Sbraccia, Sandro Scandolo, Gabriele Sclauzero, Ari P Seitsonen, Alexander Smogunov, Paolo Umari, and Renata M Wentzcovitch. *J. Phys. Condens. Matter*, 21(39):395502, 2009.
[13] R.F.W Bader. *Atoms in molecules: A quantum theory.* Clarendon Press, Oxford, 1990.
[14] V. L. Moruzzi and P. M. Marcus. *Phys. Rev. B*, 46:3171, 1992.
[15] Jürgen Kübler. *Theory of Itinerant Magnetism.* Clarendon Press, Oxford, 2000.
[16] J. Enkovaara, D. Wortmann, and S. Blügel. *Phys. Rev. B*, 76:054437, 2007.
[17] R. Soulairol, Chu-Chun Fu, and C. Barreteau. *Phys. Rev. B*, 84:155402, 2011.
[18] A. Eichler and J. Hafner. *Phys. Rev. B*, 62:5163, 2000.
[19] T. Ossowski and A. Kiejna. *Surf. Sci.*, 602:517, 2008.
[20] R. Hafner, D Spišák, R. Lorenz, and J. Hafner. *Phys. Rev. B*, 65:184432, 2002.
[21] D. Wortmann, S. Heinze, P. Kurz, G. Bilhmayer, and S.. Blügel. *Phys. Rev. Lett.*, 86:4132, 2001.
[22] S.L. Kawahara, J. Lagoute, V. Repain, S. Chacon, C.and Rousset, Y. Girard, A. Smogunov, and C. Barreteau. *Nano Lett.*, 12:4558, 2012.
[23] R. Gebauer. *Nouvelles méthodes pour le calcul ab-initio des propriétés statiques et dynamiques des matériaux magnétiques.* PhD thesis, Ecole Normale Suprieure de Lyon, 1999.
[24] J. Lagoute, S.L. Kawahara, C. Chacon, V. Repain, and Y. Girard. *J. Phys. Condens. Matter*, 23:045007, 2011.

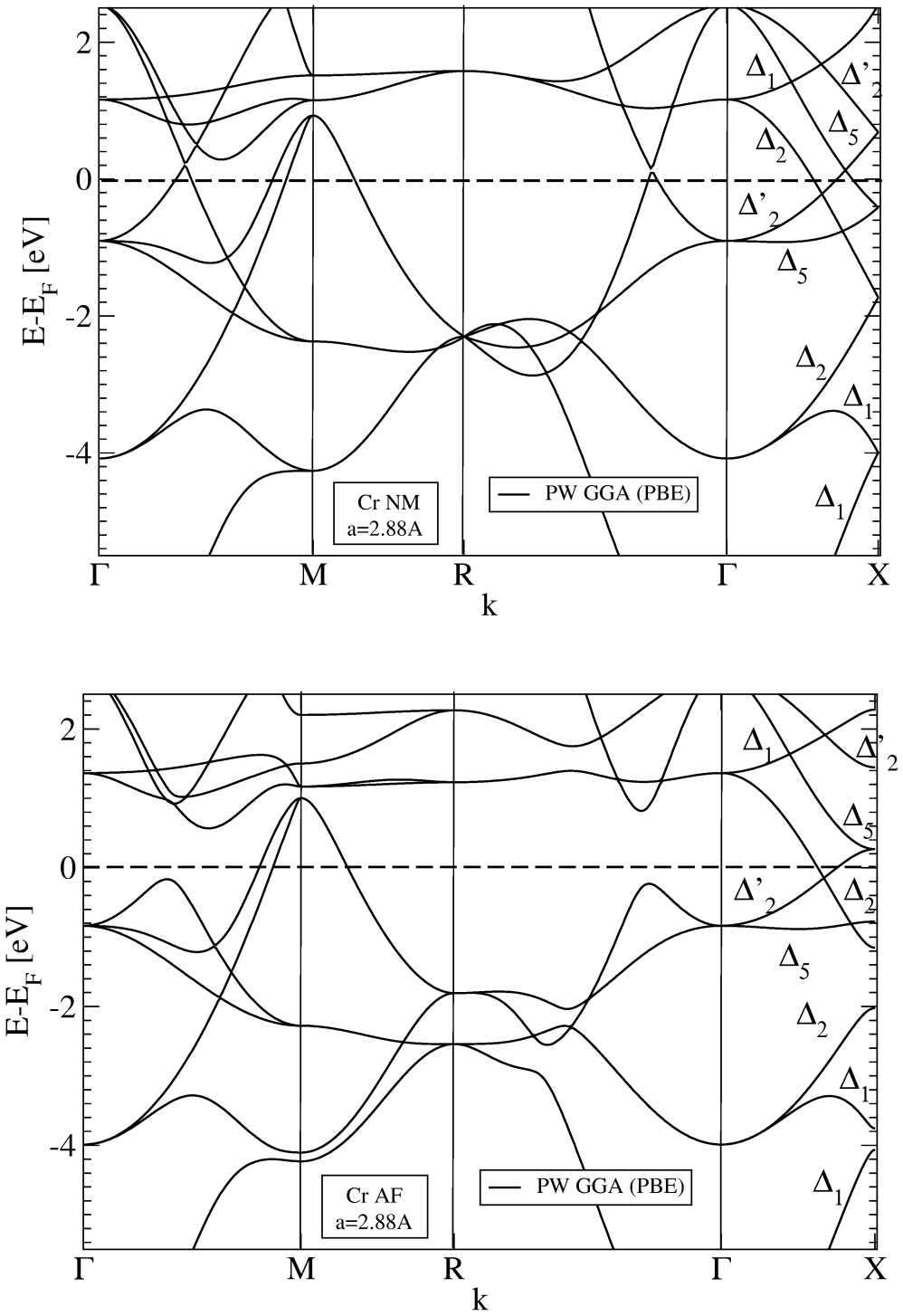

Figure 1. Top panel: Band structure of bulk non magnetic Chromium folded into the Brillouin zone of the CsCl structure. Bottom panel: Band structure of bulk antiferromagnetic Chromium in CsCl cell.

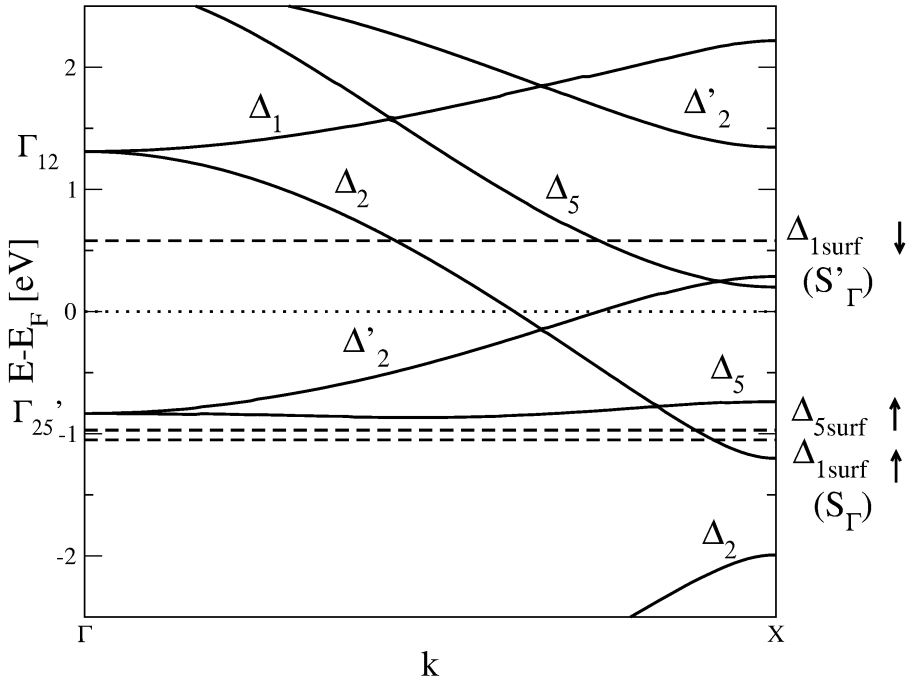

Figure 2. (Color online) Band structure of the bulk anti-ferromagnetic Chromium in CsCl cell along the $\Gamma - X$ line in the vicinity of the Fermi level. The position of the three surface states at the $\overline{\Gamma}$ point (discussed in the text) is shown. We have labeled the bands by their symmetry character along the Δ line

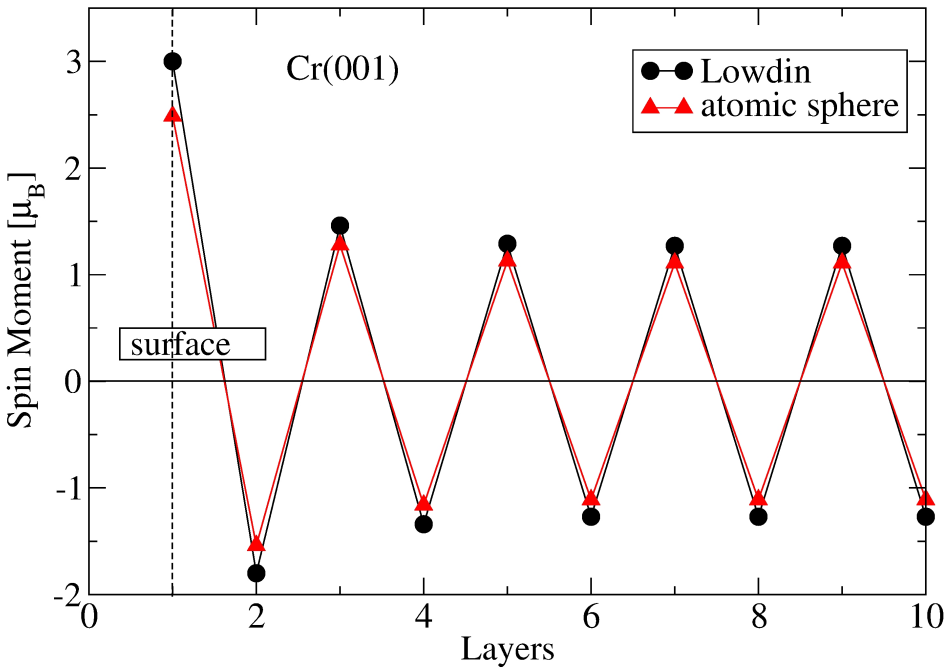

Figure 3. (Color online) Variation of the spin magnetic moment per atom on successive layers of the Cr(001) surface for two alternative definitions of the local magnetic moment: spin density integrated inside an atomic sphere or Löwdin formulation.

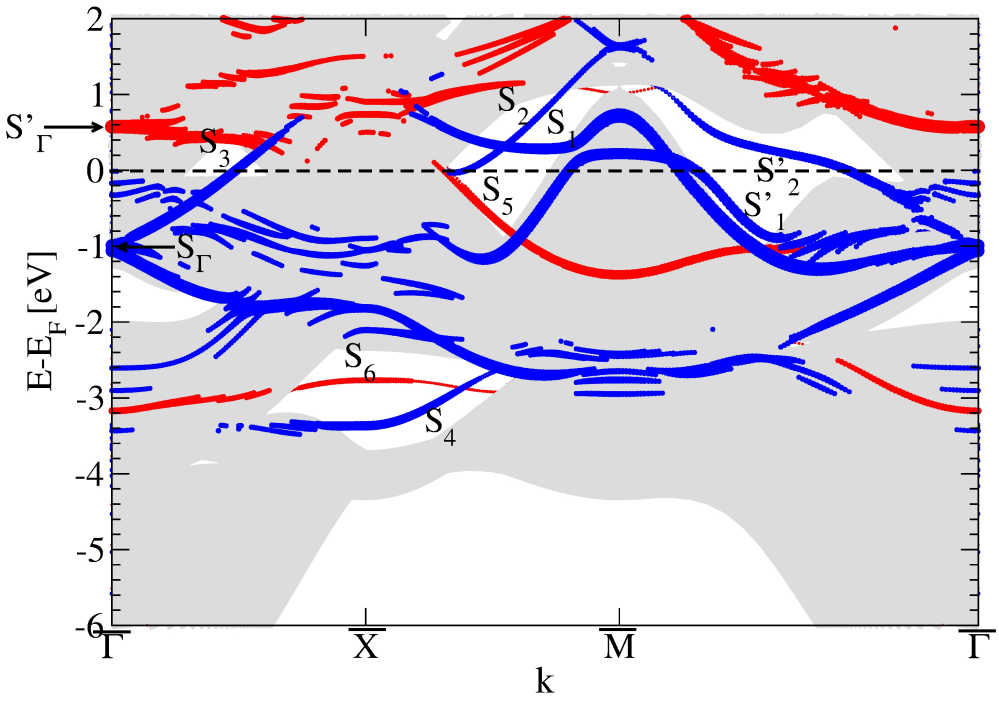

Figure 4. (Color online) Surface band structure for up (blue) and down (red) spins obtained from calculations on an 19-layer (001) slab of anti-ferromagnetic chromium at the experimental lattice parameter of 2.88Å. The size of the dots is proportional to the total weight ($s+p+d$) of the wave-functions on the outermost surface layer (bands with a total weight below 0.12 are ignored).

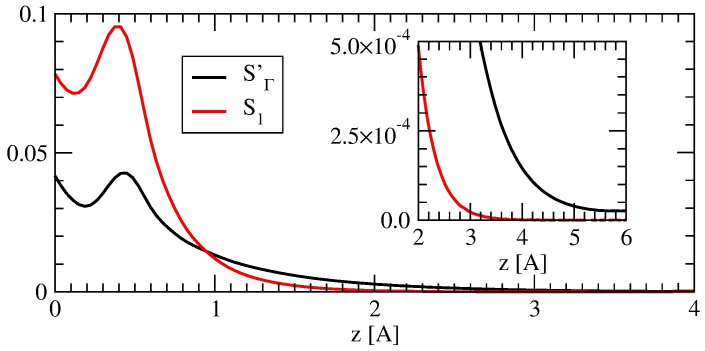

Figure 5. Square of the Bloch wave function $|\Psi^n_k(0,0,z)|^2$ along a line perpendicular to the surface, orginating from a surface atom at $z=0$ and going away into the vacuum ($z>0$). Two Bloch function are considered: a first one corresponding to the surface state S'_Γ ($k=(0,0,0)$) and another one to the surface state S_1 ($k=2\pi/a(0.5,0.3,0)$). In the inset we have shown a zoom of the same curve for distances beyond two Angstrom showing the different decay of the two surface states.

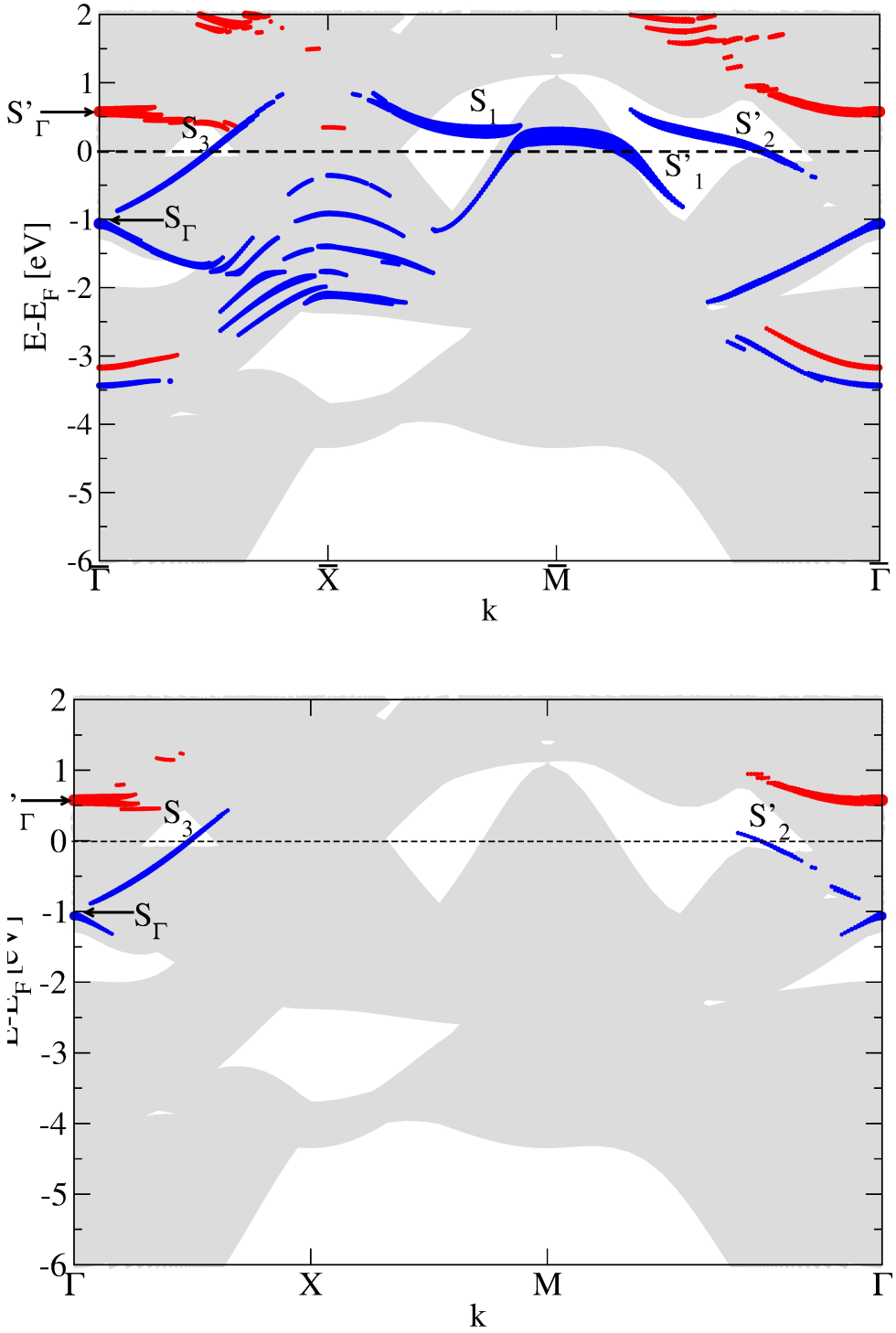

Figure 6. (Color online) Orbital-projected band structure for up (blue) and down (red) spins of a 19 layer (001) slab of anti-ferromagnetic chromium at the experimental lattice parameter of 2.88Å. The size of the dots is proportional to the weight of the component of the eigenfunction on the corresponding surface orbital (bands with a weight below 0.06 are ignored). Top: Projection on d_{z^2} orbitals. Bottom: Projection on p_z orbitals. The most important surface states for each orbital are indicated. In gray we have superimposed the corresponding surface adapted projected bulk band structure.

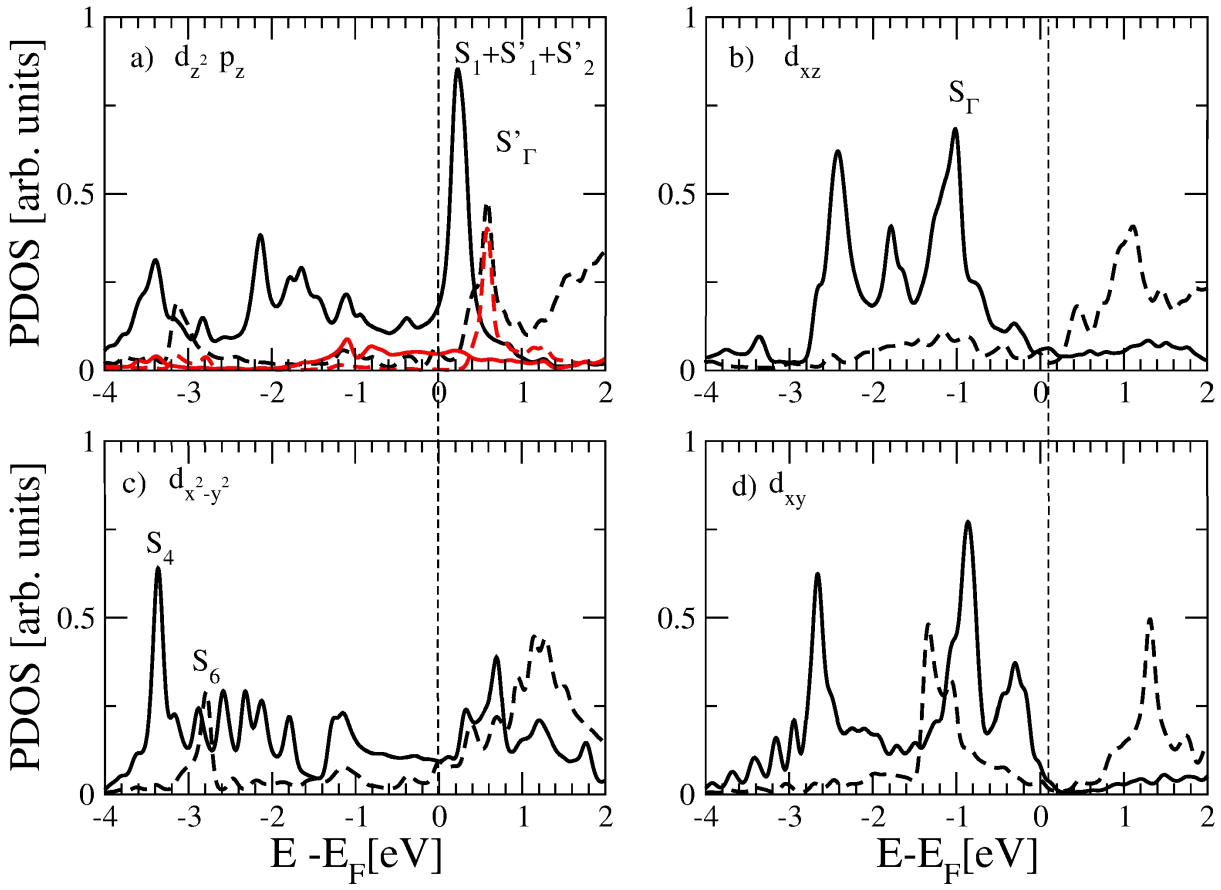

Figure 7. (Color online) Spin and orbital resolved PDOS of the (001) surface of antiferromagnetic chromium projected on a) d_{z^2} (black-line)-p_z (red line), b) d_{xz} (d_{yz}), c) $d_{x^2-y^2}$, d) d_{xy} orbital of the outermost surface site. Spin "up" is represented in full line and spin "down" in dashed line.

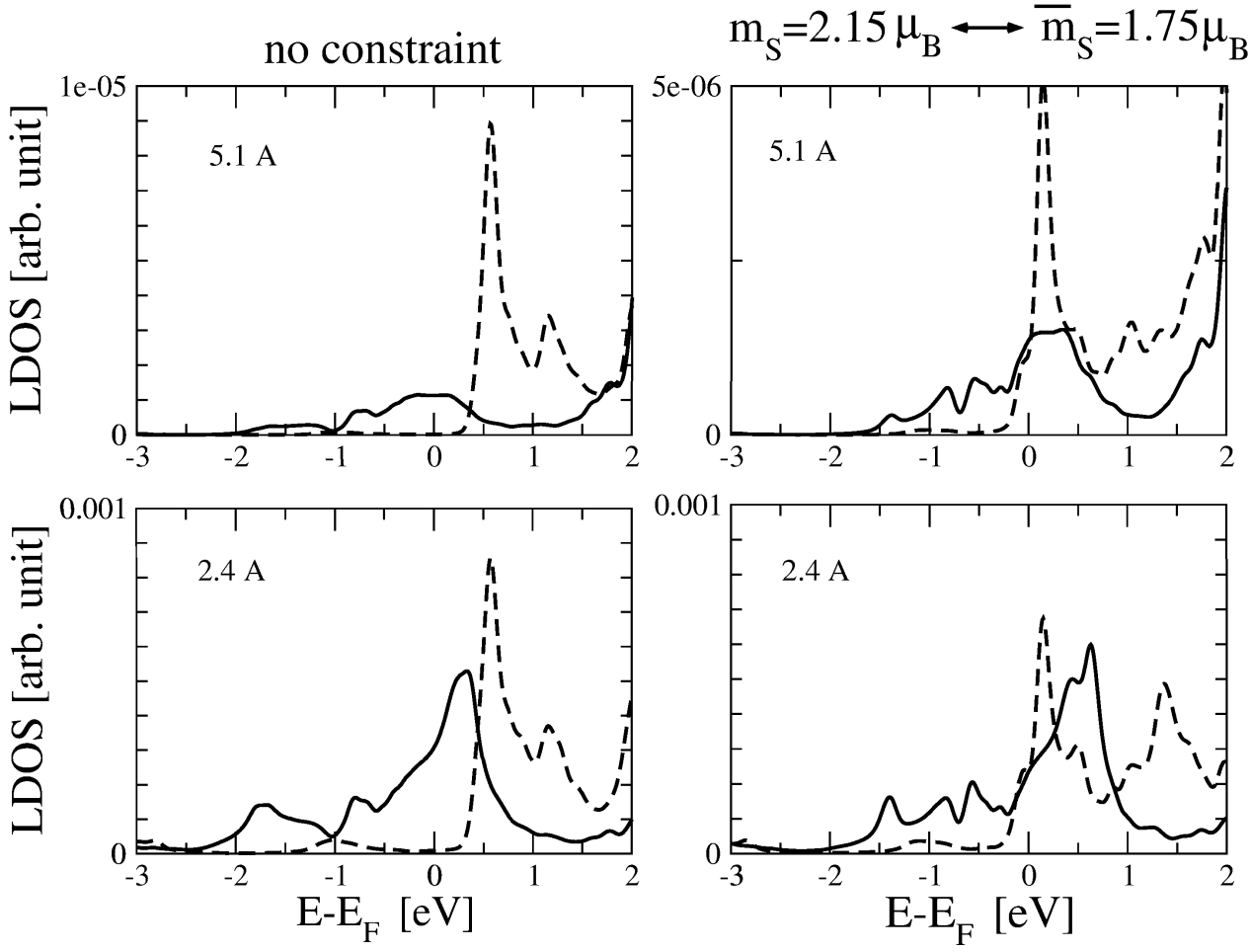

Figure 8. Spin resolved LDOS in the vacuum of the (001) surface of anti-ferromagnetic Chromium at $z = 2.4\mathring{A}$ and $z = 5.1\mathring{A}$ above the surface atom. Left panels: DFT calculation without any constraint on the magnetization (surface magnetic moment in a sphere $\overline{m}_S = 2.49\mu_B$ and with Löwdin definition $m_S = 3\mu_B$). Right panels: DFT calculations where the magnetization of the surface outermost atom is constrained to a value of $\overline{m}_S = 1.75\mu_B$, the corresponding surface Löwdin moment m_S is found to be equal to $2.15\mu_B$ Spin "up" is represented in full line and spin "down" in dashed line.